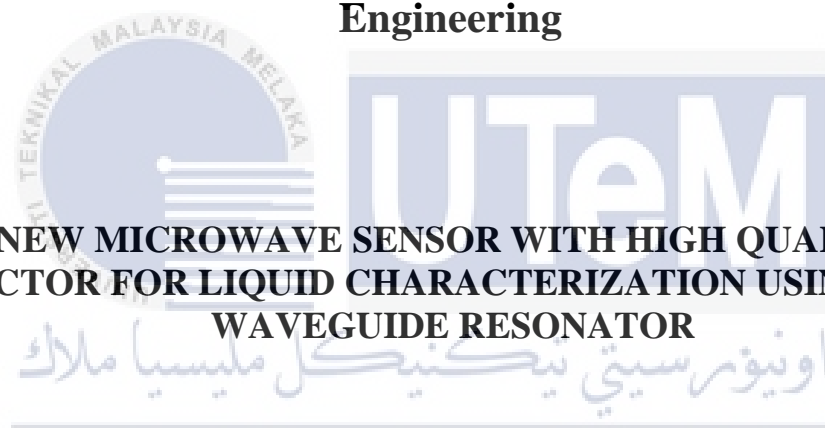




**Faculty of Electronics and Computer Technology and
Engineering**



**NEW MICROWAVE SENSOR WITH HIGH QUALITY
FACTOR FOR LIQUID CHARACTERIZATION USING GAP
WAVEGUIDE RESONATOR**

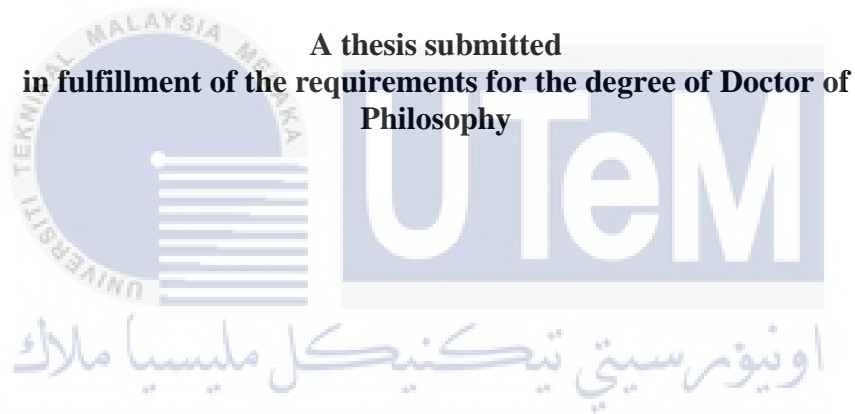
Ammar Abdullah Hussein Al-Hegazi

Doctor of Philosophy

2024

**NEW MICROWAVE SENSOR WITH HIGH QUALITY FACTOR FOR LIQUID
CHARACTERIZATION USING GAP WAVEGUIDE RESONATOR**

AMMAR ABDULLAH HUSSEIN AL-HEGAZI



Faculty of Electronics and Computer Technology and Engineering

UNIVERSITI TEKNIKAL MALAYSIA MELAKA

2024

DEDICATION

To my beloved mother and father



ABSTRACT

Characterization of material properties is crucial for facilitating a wide range of industrial applications, notably in food processing, bioengineering, and the pharmaceutical industry. Each material exhibits specific electrical behaviors influenced by its dielectric properties. Traditionally, material characterization has been conducted using conventional waveguides, such as rectangular waveguide cavities and horn antenna waveguides. However, these traditional resonators are typically large and complex to manufacture. Consequently, most researchers prefer planar structures, such as microstrip structures, for material sensing due to their simplicity and low cost. Despite these advantages, planar resonators are susceptible to external factors like oxidation and electromagnetic (EM) waves, leading to low sensitivity and Q-factor. Moreover, most microwave sensors are limited to detecting changes in liquid mixtures only when the changes exceed 10%; smaller changes go undetected. In response to these challenges, this research proposes a new microwave sensor with high sensitivity and quality factor, based on a gap waveguide resonator operating at 5.8 to 6.2 GHz for liquid characterization. Different types of liquids are analyzed and evaluated both in electromagnetic simulations and laboratory experiments using the proposed gap waveguide sensor (GWS). The gap waveguide was chosen for its ability to effectively concentrate the electric field, resulting in a high quality factor (Q-factor) and enhanced sensitivity. The liquid under test (LUT) is positioned in the region where the electric field is concentrated, allowing interaction between the electric field and the liquid material according to the principles of perturbation theory. The equations for the dielectric properties of the unknown LUT are extracted using the polynomial fitting method and Cramer's rule. The proposed sensor is simulated using Computer Simulation Technology (CST) and fabricated with a CNC machine. Experimental measurements and validation of the proposed sensor are performed in the laboratory using a Vector Network Analyzer (VNA) and the dielectric probe from Keysight. These measurements revealed a notably high quality factor of 6016. Various liquid materials, including chemical solutions and oils, were tested using the proposed sensor. The results demonstrated the sensor's remarkable sensitivity, capable of detecting even 1% changes in the mixture of ethanol and distilled water. A comparison between simulated and measured outcomes indicated strong agreement between the two data sets. The experiment showed that the proposed sensor could differentiate between different types of oils, such as virgin oil, light oil, pure oil, and used oil. The measurements using the proposed sensor showed good agreement with the dielectric probe from Keysight Technologies, with an accuracy of up to 99.65%. A comparison between the proposed sensor and recently reported research indicated that the proposed sensor has the highest quality factor. Therefore, the proposed sensor is reliable and a strong candidate for industrial applications, such as food processing, bioengineering, and the pharmaceutical industry.

PENDERIA GELOMBANG MIKRO BAHARU DENGAN FAKTOR KUALITI TINGGI UNTUK PENCIRIAN CECAIR MENGGUNAKAN PENYALUN SELA PANDU GELOMBANG

ABSTRAK

Pencirian sifat bahan menjadi penting dalam memudahkan pelbagai aplikasi industri, terutamanya dalam bidang seperti pemprosesan makanan, kejuruteraan bio dan industri farmaseutikal. Setiap bahan mempunyai tingkah laku elektrik tertentu yang dipengaruhi oleh sifat dielektriknya. Pencirian bahan telah direalisasikan dengan menggunakan pandu gelombang konvensional seperti rongga pandu gelombang segi empat tepat dan pandu gelombang antena tanduk. Walau bagaimanapun, penyalun tradisional ini biasanya bersaiz besar dan kompleks untuk dihasilkan. Oleh itu, kebanyakan penyelidik cenderung menggunakan struktur satah seperti struktur jalur mikro untuk penderiaan bahan kerana kelebihannya seperti kesederhanaan dan kos rendah. Walau bagaimanapun, penyalun ini dipengaruhi oleh faktor luaran seperti pengoksidaan dan gelombang Elektromagnet (EM) disebabkan oleh strukturnya yang membawa kepada kepekaan rendah dan faktor Q. Selain itu, kebanyakan penderia gelombang mikro terhad untuk merasakan perubahan dalam cecair campuran dengan perubahan sebanyak 10% sahaja, oleh itu perubahan kecil dalam bahan kurang daripada 10% tidak akan dikesan oleh penderia ini. Sebagai tindak balas kepada cabaran ini, objektif penyelidikan ini adalah untuk mencadangkan penderia gelombang mikro baharu dengan kepekaan tinggi dan faktor kualiti berdasarkan penyalun pandu gelombang jurang pada 5.8 hingga 6.2 GHz untuk pencirian cecair. Jenis cecair yang berbeza dianalisis dan dinilai dalam simulasi dan makmal Elektromagnet menggunakan pengesanan pandu gelombang jurang (GWS) yang dicadangkan. Pilihan pandu gelombang jurang untuk penyelidikan ini adalah berdasarkan keupayaannya untuk menumpukan medan elektrik dengan berkesan, yang membawa kepada faktor kualiti tinggi (faktor Q) dan meningkatkan sensitiviti. Cecair dalam ujian (LUT) diletakkan di kawasan di mana medan elektrik tertumpu. Susunan ini membolehkan interaksi antara medan elektrik dan bahan cecair, mengikut prinsip teori gangguan. Persamaan untuk sifat dielektrik LUT yang tidak diketahui diekstrak menggunakan kaedah pemasangan polinomial dan peraturan Cramer. Penderia yang dicadangkan disimulasikan menggunakan Teknologi Simulasi Komputer (CST) dan direka menggunakan mesin CNC. Pengukuran eksperimen dan pengesanan penderia yang dicadangkan dilakukan di makmal menggunakan Penganalisis Rangkaian Vektor (VNA) dan kuar dielektrik dari Keysight. Pengukuran ini mendedahkan faktor kualiti yang sangat tinggi iaitu 6016. Pelbagai bahan cecair, termasuk larutan kimia dan minyak, diuji menggunakan penderia yang dicadangkan. Hasilnya menunjukkan sensitiviti luar biasa penderia, mampu mengesan walaupun 1% perubahan dalam campuran etanol dan air suling. Perbandingan antara hasil simulasi dan diukur menunjukkan persetujuan yang kukuh antara dua set data. Eksperimen menunjukkan bahawa penderia yang dicadangkan boleh membezakan antara pelbagai jenis minyak seperti minyak dara, minyak ringan, minyak tulen dan minyak terpakai. Pengukuran menggunakan penderia yang dicadangkan menunjukkan persetujuan yang baik dengan kuar dielektrik dari Keysight Technologies dengan ketepatan sehingga 99.65%. Perbandingan antara penderia yang dicadangkan dan penyelidikan yang dilaporkan baru-baru ini menunjukkan bahawa penderia yang dicadangkan mempunyai faktor kualiti tertinggi. Oleh itu, penderia yang dicadangkan boleh dipercayai dan calon yang baik untuk aplikasi industri seperti pemprosesan makanan, biokejuruteraan dan industri farmaseutikal.

ACKNOWLEDGEMENTS

I would like to begin by extending my heartfelt gratitude and sincere acknowledgment to my supervisor, Dr. Noor Azwan Bin Shairi, affiliated with the Faculty of Electronic and Computer Engineering at Universiti Teknikal Malaysia Melaka (UTeM). His invaluable supervision, unwavering support, guidance, and consistent encouragement have been pivotal in steering this thesis to successful completion.

I would also like to convey my utmost gratitude to Prof. Dr. Zahriladha Bin Zakaria, a co-supervisor and project leader of this research project hailing from the Faculty of Electronic and Computer Engineering. His crucial supervision, unwavering support, patient guidance, invaluable suggestions, and his willingness to generously dedicate his time have all been deeply appreciated throughout this research endeavor.

I extend my special thanks to the UTeM short-term grant for providing the necessary financial support throughout this project. Additionally, I would like to express my heartfelt gratitude to Mr. Mohd Sufian Bin Abu Talib, the technician from the measurement laboratory of the Faculty of Electronic and Computer Engineering, for his invaluable assistance and support.

Another great appreciation to my beloved mother, father and siblings for their support and encouragement in completing this degree.

Particularly, I wish to thank various people; Dr. Rammah Al-Alahnomi, Dr. Hussein Alsarayra, Dr. Amyrul Azuan Mohd Bahar, Dr. Sam Weng Yik, Dr. Norhanani Abd Rahman and Mr. Husam Alwareth for their valuable technical support of this research.

I would like to extend my gratitude to the department and faculty members for their assistance and support during this research. Additionally, I am thankful to my friends who provided me with support throughout this endeavor. Your encouragement and help have been greatly appreciated.

TABLE OF CONTENTS

| | PAGE |
|---|-----------|
| DECLARATION | |
| APPROVAL | |
| DEDICATION | |
| ABSTRACT | i |
| ABSTRAK | ii |
| ACKNOWLEDGEMENTS | iii |
| TABLE OF CONTENTS | iv |
| LIST OF TABLES | vii |
| LIST OF FIGURES | x |
| LIST OF ABBREVIATION | xviii |
| LIST OF SYMBOLS | xxi |
| LIST OF APPENDICES | xxiii |
| LIST OF PUBLICATIONS | xxiv |
| AWARD | xxv |
| | |
| CHAPTER | |
| 1. INTRODUCTION | 1 |
| 1.1 Research Background | 1 |
| 1.2 Problem Statement | 5 |
| 1.3 Research Objectives | 7 |
| 1.4 Scope of Research | 8 |
| 1.5 Contributions | 9 |
| 1.6 Thesis Organization | 10 |
| | |
| 2. LITERATURE REVIEW | 13 |
| 2.1 Introduction | 13 |
| 2.2 Fundamentals of Rectangular Waveguide Resonator | 13 |
| 2.2.1 Basic Theory of Parallel Plate Waveguide Resonator | 17 |
| 2.2.2 Mathematical Model of TM Modes | 18 |
| 2.2.3 Impedance matching (Newton boundary condition) | 21 |
| 2.3 Waveguides and Transmission Lines Technologies | 21 |
| 2.3.1 Planar Waveguides | 22 |
| 2.3.2 Hollow Waveguides and Substrate Integrated Waveguides | 24 |
| 2.4 Gap Waveguide Technology | 26 |
| 2.5 Microwave Sensing Methods | 33 |
| 2.5.1 Non-Resonant Method | 35 |
| 2.5.1.1 Reflection Method | 39 |
| 2.5.1.2 Transmission Line Method | 43 |
| 2.5.1.3 Shorted Reflection Method | 47 |
| 2.5.1.4 Free Space Method | 48 |
| 2.5.2 Resonant Method | 50 |
| 2.5.2.1 Resonant Cavities | 53 |
| 2.5.2.2 Dielectric Resonator | 54 |
| 2.5.2.3 Planar Lines Resonator | 55 |
| 2.6 Microwave Resonator | 59 |
| 2.6.1 Resonant Frequency | 60 |
| 2.6.2 Equivalent Circuits | 62 |

| | | |
|-----------|---|------------|
| 2.7 | Design of Microwave Resonator | 63 |
| 2.8 | General Properties of Materials | 65 |
| 2.9 | Material Characterization | 68 |
| 2.10 | Microwave Sensing Strategies | 70 |
| 2.11 | Derivation of Equations using Cramer's Rule | 72 |
| 2.12 | Popular Microwave Techniques for Material Properties Characterization | 76 |
| 2.12.1 | Planar Resonators | 76 |
| 2.12.2 | Co-Planar Waveguide (CPW) | 85 |
| 2.12.3 | Substrate Integrated Waveguide (SIW) | 86 |
| 2.12.4 | Metal Waveguide | 88 |
| 2.12.5 | Comparison of Recent Developments in Microwave Resonators | 93 |
| 2.13 | Summary | 98 |
| 3. | RESEARCH METHODOLOGY | 101 |
| 3.1 | Introduction | 101 |
| 3.2 | Flow Chart | 101 |
| 3.3 | Mathematical Model | 105 |
| 3.3.1 | LC equivalent circuit | 105 |
| 3.3.2 | Quality Factor | 108 |
| 3.4 | Electromagnetic Field | 110 |
| 3.5 | Basic Design of Gap Waveguide | 112 |
| 3.5.1 | Design of Gap Waveguide with One Port | 113 |
| 3.5.1.1 | Gap Waveguide with One Port on the Upper Plate | 113 |
| 3.5.1.2 | Gap Waveguide with One Side Port | 114 |
| 3.5.1.3 | Gap Waveguide Sensor with MUT | 116 |
| 3.5.2 | Design of Gap waveguide with Two Ports | 117 |
| 3.6 | Design of Gap Waveguide Sensor for Liquid Characterization | 119 |
| 3.7 | Equation Extraction | 122 |
| 3.8 | Manufacturing | 124 |
| 3.9 | Measurement | 124 |
| 3.10 | Summary | 126 |
| 4. | GAP WAVEGUIDE SENSOR | 128 |
| 4.1 | Introduction | 128 |
| 4.2 | Simulation Results of Basic Design of Gap Waveguide Sensor | 128 |
| 4.2.1 | Gap Waveguide with One Port | 128 |
| 4.2.2 | Gap Waveguide with One Port and MUT | 130 |
| 4.3 | Simulation Results of Gap Waveguide Sensor | 131 |
| 4.3.1 | Gap Waveguide Sensor with and without Cavity | 131 |
| 4.3.2 | Parametric Study of Gap Waveguide Sensor | 132 |
| 4.4 | Comparison of the Simulation and Measurement Results | 136 |
| 4.4.1 | Transmission Coefficient | 136 |
| 4.4.2 | Equation Extraction | 138 |
| 4.4.3 | Sensitivity | 142 |
| 4.4.4 | Verification of the Evaluated Values | 143 |
| 4.5 | Summary | 145 |
| 5. | ENHANCED GAP WAVEGUIDE SENSOR | 147 |

| | | |
|-----------|--|------------|
| 5.1 | Introduction | 147 |
| 5.2 | Simulations and Optimizations | 147 |
| 5.2.1 | Parametric Study for Permittivity and Loss Tangent | 148 |
| 5.2.1 | Relationship between Dielectric Constant and Dielectric Loss | 152 |
| 5.3 | Comparison of the Simulation and Measurement Results | 157 |
| 5.3.1 | Transmission Coefficient | 157 |
| 5.3.2 | Equation Extraction | 161 |
| 5.3.3 | Sensitivity | 165 |
| 5.4 | Concentration Measurement | 166 |
| 5.4.1 | Ethanol Solution | 166 |
| 5.4.2 | Olive Oil | 168 |
| 5.4.3 | Sunflower Oil | 170 |
| 5.5 | Relationship between the Volume of the LUT and Frequency Shift | 171 |
| 5.6 | Comparison of the Proposed Sensor with Recently Reported Results | 175 |
| 5.7 | Summary | 179 |
| 6. | CONCLUSION AND SUGGESTIONS FOR FUTURE WORK | 180 |
| 6.1 | Conclusion | 180 |
| 6.2 | Future Works | 181 |
| | REFERENCES | 185 |
| | APPENDICES | 218 |



اونيورسيتي تيكنيكل مليسيا ملاك

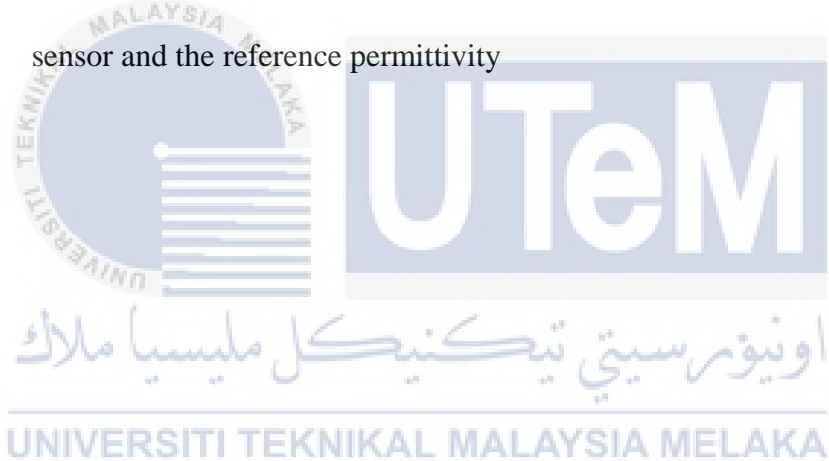
UNIVERSITI TEKNIKAL MALAYSIA MELAKA

LIST OF TABLES

| TABLE | TITLE | PAGE |
|-------|---|------|
| 2.1 | Comparison of the microwave sensing methods | 33 |
| 2.2 | Comparison of material properties and transmission line with different methods | 34 |
| 2.3 | Design specifications of the proposed sensor | 64 |
| 2.4 | Different characteristics of the material physical phenomena under the applied electric field | 66 |
| 2.5 | Comparison of sensing strategies | 71 |
| 2.6 | Comparison of Recent Developments in Microwave Sensors | 93 |
| 2.7 | Comparison between the recent microwave sensors in terms of sensitivity and concentration percentage | 94 |
| 2.8 | Comparison between the recent microwave sensors | 97 |
| 3.1 | The details of simulation conditions | 112 |
| 4.1 | Design parameters values of the proposed sensor | 133 |
| 4.2 | The relationship between the permittivity, resonant frequency, and frequency shift | 135 |
| 4.3 | Comparison of the extracted values for permittivity and loss tangent using polynomial fitting curve and Cramer's rule | 141 |
| 4.4 | Comparison of the proposed sensor with recently reported results | 142 |

| | | |
|------|---|-----|
| 4.5 | Comparison of the proposed sensor with commercialized sensors for ethanol and methanol at 6.1 GHz | 145 |
| 5.1 | Parametric study for the permittivity with the loss tangent of the air | 149 |
| 5.2 | Parametric study for the loss tangent from 0.02 to 1 with increment of 0.0408 and permittivity of the air | 151 |
| 5.3 | Parametric study for the permittivity and loss tangent | 154 |
| 5.4 | Relationship between the bandwidth, loss tangent and quality factor | 156 |
| 5.5 | Comparison of the simulated and measured results of the proposed sensor with and without LUT | 161 |
| 5.6 | Comparison of the measured results of proposed sensor with the dielectric probe from Keysight Technologies | 163 |
| 5.7 | Comparison of the proposed sensor with commercialized sensors for ethanol and methanol at 6.1 GHz | 163 |
| 5.8 | Comparison of the proposed sensor with other recently reported sensors for methanol using the graph from Keysight technologies in Figure 5.13 | 165 |
| 5.9 | Comparison of the proposed sensor with reported researches in terms of, structure, frequency, frequency shift and sensitivity | 165 |
| 5.10 | Comparison of the dielectric constant and dielectric loss with different concentration percentages | 167 |
| 5.11 | Comparison of the measured S_{21} for olive oil with different concentrations in terms of energy and fat | 170 |

| | | |
|------|--|-----|
| 5.12 | Comparison of the measured S_{21} for sunflower oil with different concentrations | 171 |
| 5.13 | Comparison of the proposed sensor with different diameters of Teflon tube for castor oil and ethanol | 173 |
| 5.14 | Comparison between the GWS and the enhanced GWS | 175 |
| 5.14 | Comparison between the recent microwave sensors in terms of sensitivity and concentration percentage | 176 |
| 5.15 | Comparison of the proposed sensor with the recent methods for liquid characterization | 177 |
| 6.1 | Comparison between the evaluated permittivity by the proposed sensor and the reference permittivity | 184 |



LIST OF FIGURES

| FIGURE | TITLE | PAGE |
|--------|---|------|
| 1.1 | Gap waveguide geometries: (a) Ridge gap waveguide, (b) Groove gap waveguide, (c) Inverted- microstrip gap waveguide, (d) Microstripridge gap waveguide (Zaman and Glazunov, 2017) | 5 |
| 2.1 | Parallel plate waveguide | 18 |
| 2.2 | (a) Microstrip line, (b) suspended microstrip line (c) coplanar waveguides and (d) grounded coplanar waveguides | 23 |
| 2.3 | (a) Hollow rectangular waveguide and (b) substrate integrated waveguide | 25 |
| 2.4 | Principle of operation of the gap waveguide | 27 |
| 2.5 | Front view of the ridge gap waveguide | 28 |
| 2.6 | Gap waveguide geometries: (a) Ridge gap waveguide, (b) Groove gap waveguide, (c) Inverted- microstrip gap waveguide, (d) Microstripridge gap waveguide (Zaman and Glazunov, 2017) | 29 |
| 2.7 | Diagram of the ridge gap waveguide | 29 |
| 2.8 | Groove gap waveguide | 30 |
| 2.9 | HIS produced by the surface of pins | 31 |
| 2.10 | HIS produced by mushroom shape surface inserted in dielectric | 31 |
| 2.11 | Strip and mushroom surface have the same substrate | 31 |

| | | |
|------|--|----|
| 2.12 | Slot antenna in ridge gap waveguide technology (Zaman and Kildal, 2012) | 32 |
| 2.13 | Gap waveguide for millimetre-wave systems: (a) Coupler prototype, (b) Filter prototype (Alfonso et al., 2012) | 32 |
| 2.14 | Material characterization using non-resonant method (Chen et al., 2004) | 35 |
| 2.15 | Incident, transmitted and reflected electromagnetic waves in a filled transmission line (Shukla, 2015) | 37 |
| 2.16 | Transmission line methods (a) Sample inside the coaxial line (b) Sample inside the waveguide line (Costa et al., 2017) | 38 |
| 2.17 | Diagram of the principles of the reflection method | 39 |
| 2.18 | Operation principles of the open ended coaxial | 40 |
| 2.19 | Open-ended coaxial line (Vergnano et al., 2020) | 41 |
| 2.20 | Open-ended coaxial line (Li et al., 2021) | 41 |
| 2.21 | Olive oil characterization using rectangular waveguide probe (Sahin, Nahar and Sertel, 2020) | 43 |
| 2.22 | Diagram of material characterization using coaxial line (Karuppuswami et al., 2018) | 44 |
| 2.23 | Diagram of the waveguide transmission line for material characterization (Ahmad et al., 2015) | 45 |
| 2.24 | Planar transmission line with PDMS (Jasińska and Malecha, 2021) | 46 |
| 2.25 | Coplanar sensor using IDC (Chen et al., 2012) | 47 |
| 2.26 | Coaxial short circuit reflection (Chen et al., 2004) | 48 |
| 2.27 | Free space measurement setup using VNA (Wee et al., 2009) | 49 |

| | | |
|------|--|----|
| 2.28 | Classification of resonator methods for the study of dielectric properties of low-loss samples (Chen et al., 2004) | 51 |
| 2.29 | Diagram of the cavity resonator with sample | 53 |
| 2.30 | Microwave sensor using dielectric resonator (Neshat et al., 2010) | 54 |
| 2.31 | Microwave sensor using dielectric resonator (a) simulation and (b) measurement (Taeb et al., 2011) | 55 |
| 2.32 | Electric field of the microstrip (Al-Nuaimi and Whittow, 2010) | 56 |
| 2.33 | Planar line resonator sensor (Jean, Green and McClung, 2008) | 56 |
| 2.34 | Coplanar sensor using IDC (Crupi et al., 2020) | 57 |
| 2.35 | Transmission line sensor (a) diagram and (b) measurement (Meyne et al., 2015) | 58 |
| 2.36 | Microwave sensor using filter stub resonator (a) diagram and (b) diagram of measurement set up (Pinon et al., 2012) | 59 |
| 2.37 | Cross section of the microstrip substrate (a) designed and (b) manufactured (Pinon et al., 2012) | 59 |
| 2.38 | Typical response (S_{21}) of power transmission of the resonator with and without a sample (A. A. Abduljabar et al., 2014) | 61 |
| 2.39 | Equivalent circuits (a) Series equivalent RLC (b) Parallel equivalent RLC | 62 |
| 2.40 | Parallel equivalent circuit of the resonator | 62 |
| 2.41 | Two ports network (Hong and Lancaster, 2004) | 64 |
| 2.42 | Fabricated BMSRR (Amyrul Azuan Mohd Bahar et al., 2017) | 79 |
| 2.43 | Measured and simulated results of the BMSRR with different types of liquid (Amyrul Azuan Mohd Bahar et al., 2017) | 79 |
| 2.44 | Planar T-shape resonator (Sandhu, Hunter and Roberts, 2016) | 80 |

| | | |
|------|---|-----|
| 2.45 | Planar coupled resonators (Coutinho et al., 2018) | 81 |
| 2.46 | Planar coupled resonators with sample (Coutinho et al., 2018) | 81 |
| 2.47 | Fabricated IDE sensor (Fok et al., 2015) | 82 |
| 2.48 | Measured results using IDE sensor (Fok et al., 2015) | 83 |
| 2.49 | Microstrip patch antenna (Cheng et al., 2014) | 84 |
| 2.50 | Measured results of the reflection coefficient with a percentage of salt content in the solution (Cheng et al., 2014) | 85 |
| 2.51 | Microwave co-planar sensor (Mason et al., 2013) | 86 |
| 2.52 | Substrate integrated Cavity (Ndoye et al., 2017) | 87 |
| 2.53 | Measured results of resonant frequency as a function of the humidity variation (Ndoye et al., 2017) | 88 |
| 2.54 | Fabricated sensor using nano-fluidic millimetre waveguide (Chudpooti et al., 2018) | 89 |
| 2.55 | Measured results of the microwave sensor using nano-fluidic millimetre waveguide (Chudpooti et al., 2018) | 90 |
| 2.56 | Cylindrical cavity microwave sensor (Korostynska, Mason and Al-Shamma'a, 2014a) | 91 |
| 2.57 | Measured results using cylindrical cavity microwave sensor (Korostynska, Mason and Al-Shamma'a, 2014a) | 92 |
| 2.58 | Rectangular waveguide cavity with the material under test (Jha, Rahaman and Akhtar, 2014) | 92 |
| 3.1 | Flow chart of the research | 104 |
| 3.2 | Diagram of the LC equivalent circuit for the GWR | 105 |
| 3.3 | Geometrical diagram of the principle of operation of the proposed GWR | 106 |

| | | |
|------|--|-----|
| 3.4 | Expected transmission coefficient response with and without a sample (A. A. Abduljabar et al., 2014) | 109 |
| 3.5 | The electromagnetic (a) Q-TEM mode in ridge gap waveguide, (b) TE ₁₀ mode in groove gap waveguide, (c) Q-TEM mode in inverted-microstrip gap waveguide and (d) Q-TEM mode in microstrip ridge gap waveguide | 111 |
| 3.6 | Basic structure of gap waveguide sensor | 113 |
| 3.7 | Design of gap waveguide with one port on the upper plate | 113 |
| 3.8 | Design of gap waveguide with one side port | 115 |
| 3.9 | Design of gap waveguide with side port and bridge | 115 |
| 3.10 | Design of gap waveguide with tube | 117 |
| 3.11 | Design of gap waveguide with material under test | 117 |
| 3.12 | Design of gap waveguide with two ports | 118 |
| 3.13 | Design of gap waveguide with two ports at 6.1 GHz | 118 |
| 3.14 | Simulated structure of the proposed sensor | 119 |
| 3.15 | Simulated structure of the proposed sensor with capillary glass and LUT | 121 |
| 3.16 | Simulated electric field of the proposed sensor in the sensing area | 121 |
| 3.17 | Example of 2D structure of the lower plate with optimum values in millimetres using AutoCAD | 124 |
| 3.18 | Measurement setup | 125 |
| 3.19 | Working principle of the proposed sensor with LUT molecular structure | 126 |
| 4.1 | Design of gap waveguide with one side port | 129 |
| 4.2 | Design of gap waveguide with side port and bridge | 129 |

| | | |
|------|---|-----|
| 4.3 | Design of gap waveguide with single port | 129 |
| 4.4 | Simulated results of the basic design of gap waveguide sensor | 129 |
| 4.5 | Design of gap waveguide with material under test | 130 |
| 4.6 | Simulated results of the microwave sensor with a single port | 130 |
| 4.7 | Simulated electric field of the proposed sensor (a) without cavity, and (b) with cavity | 131 |
| 4.8 | Transmission coefficient of the proposed sensor with and without cavity | 132 |
| 4.9 | Transmission coefficient of the proposed sensor for varied lengths of the pins | 132 |
| 4.10 | Simulated structure of the proposed sensor | 133 |
| 4.11 | Simulated diagram of the GWR for liquid Characterization | 134 |
| 4.12 | Transmission coefficient of the proposed sensor with different values of the permittivity of the LUT | 135 |
| 4.13 | Relationship between the permittivity, frequency and frequency shift | 136 |
| 4.14 | Measurement using the proposed sensor with liquid under test | 137 |
| 4.15 | Simulated (s) and measured (m) transmission coefficient of the proposed sensor with and without LUT | 138 |
| 4.16 | Polynomial fitting curve of the permittivity | 139 |
| 4.17 | Polynomial fitting curve of the loss tangent | 140 |
| 4.18 | Relationship between the loss tangent, Q_L -factor, and transmission coefficient | 144 |
| 5.1 | Simulated structure of the proposed enhanced gap waveguide sensor | 148 |

| | | |
|------|---|-----|
| 5.2 | Parametric study for the permittivity at range from 0.5 to 12 with increment of 0.5 and loss tangent of the air | 149 |
| 5.3 | Parametric study for the loss tangent from 0.02 to 1 with increment of 0.0408 and permittivity of the air | 151 |
| 5.4 | Parametric study for the permittivity and loss tangent | 153 |
| 5.5 | Polynomial fitting curve of the permittivity and resonant frequency of the proposed sensor | 155 |
| 5.6 | Polynomial fitting curve of the loss tangent and transmission coefficient of the proposed sensor | 155 |
| 5.7 | Relationship between the frequency shift and the loss tangent of the proposed sensor | 156 |
| 5.8 | Measurement using the proposed sensor with liquid under test | 158 |
| 5.9 | Simulated (s) and measured (m) transmission coefficient of the proposed sensor with and without LUT, (a) chemical solutions and oils, (b) measured oils, (c) fish oil, (d) olive oil, (e) Linseed oil, (f) castor oil | 160 |
| 5.10 | Polynomial fitting curve of the permittivity and resonant frequency | 161 |
| 5.11 | Polynomial fitting curve of the loss tangent and transmission coefficient | 162 |
| 5.12 | Measurement using the dielectric probe from Keysight Technologies | 163 |
| 5.13 | Measured dielectric constant of methanol at a range of frequency from 0.1 to more than 10 GHz using the dielectric probe from Keysight Technologies (Keysight Technologies, 2022) | 164 |

| | | |
|------|--|-----|
| 5.14 | Measured S_{21} for ethanol with a 10% concentration increment | 167 |
| 5.15 | The relationship between loss tangent and ethanol concentration | 168 |
| 5.16 | Measured S_{21} for ethanol with 1% concentration increment | 168 |
| 5.17 | Olive oils with different concentrations | 169 |
| 5.18 | Measured S_{21} for olive oil with different concentrations | 170 |
| 5.19 | Measured S_{21} for sunflower oil with different concentrations | 171 |
| 5.20 | Measurement for the castor oil, methanol and water using (a) 1 mm Teflon tube and (b) 1.6 mm Teflon tube | 172 |
| 5.21 | Measured S_{21} for ethanol using different sizes of Teflon tube | 173 |
| 5.22 | Measured S_{21} for olive oil and seed oil using (a) 1 mm and (b) 1.6 mm Teflon tube | 174 |
| 5.23 | Measured S_{21} for olive oil and seed oil using a 2 mm Teflon tube | 174 |
| 6.1 | The enhanced GWS with 10 mm microfluidic channel | 182 |
| 6.2 | GWCR with powder under test (PUT) | 182 |
| 6.3 | Transmission coefficient of the proposed sensor with and without PUT using GWCR for powder | 183 |
| 6.4 | Polynomial graph of the permittivity | 183 |

LIST OF ABBREVIATION

| | | |
|----------|---|---|
| A-G MSRR | - | Aligned-Gap Multi-Ring Split Ring Resonator |
| AMC | - | Artificial Magnetic Conductor |
| BMSRR | - | Bridge Multiple Split Ring Resonators |
| BW | - | Bandwidth |
| C-GMSRR | - | Centered-Gap Multiple Split Ring Resonator |
| CLR | - | Coupled Line Resonator |
| Co-pol | - | Co-polarization |
| CPW | - | Coplanar Waveguide |
| CSRRs | - | Complementary Split-Ring Resonators |
| CST | - | Computer Simulation Technology |
| dB | - | Decibel |
| DSRR | - | Double Split Ring Resonator |
| E-Field | - | Electric Field |
| EM | - | Electromagnetic |
| G-CPW | - | Grounded Coplanar Waveguides |
| GHz | - | Giga Hertz |
| GW | - | Gap Waveguide |
| GWR | - | Gap Waveguide Resonator |
| HIS | - | High Impedance Surface |
| H-Field | - | Magnetic Field |
| IDC | - | Interdigitated Capacitor |

| | | |
|----------|---|----------------------------------|
| IDE | - | Interdigitated Electrode |
| IL | - | Insertion Loss |
| LUT | - | Liquid Under Test |
| M | - | Measured |
| MRR | - | Microstrip Ring Resonator |
| MUT | - | Material Under Test |
| MW | - | Microwave |
| NRW | - | Nicholson-Ross-Weir |
| NSR | - | Nonuniform Sub Resonator |
| PEC | - | Perfect Electric Conductor |
| PCB | - | Printed Circuit Board |
| PDMS | - | Polydimethylsiloxane |
| PMC | - | Perfect Magnetic Conductor |
| Q-factor | - | Quality Factor |
| Q-TEM | - | Hybrid TM-TE Wave |
| RLC | - | Resistor-Inductor-Capacitor |
| RF | - | Radio Frequency |
| Ref | - | Reference |
| RSS | - | Resonant Stub Structure |
| SIW | - | Substrate Integrated Waveguide |
| Sam | - | Sample |
| S | - | Simulated |
| SRR | - | Split Ring Resonator |
| TE | - | Transverse Electric Modes |
| TEM | - | Transverse Electric and Magnetic |

| | | |
|------|---|-----------------------------------|
| TM | - | Transverse Magnetic |
| VNA | - | Vector Network Analyze |
| VSRR | - | Vertically Stacked Ring Resonator |



LIST OF SYMBOLS

| | | |
|-------------------|---|--|
| a_n | - | Incident Wave |
| B | - | Magnetic Flux Density |
| b_n | - | Reflected Wave |
| BW | - | 3dB Bandwidth |
| c | - | Speed Of Light |
| C | - | Capacitance |
| C_l | - | Distributed Capacitance |
| D | - | Electric Flux Density |
| ϵ' | - | Real Permittivity |
| ϵ'' | - | Imaginary Permittivity |
| ϵ_∞ | - | Permittivity In The High-Frequency Limit |
| ϵ_{eff} | - | Effective Permittivity |
| ϵ_s | - | Static/Low-Frequency Permittivity |
| E | - | Electric |
| F_o | - | Resonant Frequency |
| H | - | Magnetic |
| I | - | Current |
| J | - | Electric Current Density |
| k | - | Discrete Real Numbers |
| λ | - | Wavelength |